Modeling the Endpoint Uncertainty in Crossing-based Moving Target Selection

Jin Huang[1,2] huangjin@iscas.ac.cn
Feng Tian[1,2]* tianfeng@iscas.ac.cn
Xiangmin Fan[1,2] xiangmin@iscas.ac.cn
Huawei Tu[4] h.tu@latrobe.edu.au
Hao Zhang[1,3] zhanghao181@mails.ucas.ac.cn
Xiaolan Peng[1,3] xiaolan@iscas.ac.cn
Hongan Wang[1,3] hongan@iscas.ac.cn

[1]State Key Laboratory of Computer Science and Beijing Key Lab of Human-Computer Interaction, Institute of Software, Chinese Academy of Sciences, Beijing, China
[2]School of Artificial Intelligence, University of Chinese Academy of Sciences, Beijing, China
[3]School of Computer Science and Technology, University of Chinese Academy of Sciences, Beijing, China
[4]Department of Computer Science and Information Technology, La Trobe University, Melbourne, VIC, Australia
*Corresponding author: tianfeng@iscas.ac.cn

ABSTRACT
Modeling the endpoint uncertainty of moving target selection with crossing is essential to understand factors such as speed-accuracy trade-off and interaction efficiency in crossing-based user interfaces with dynamic contents. However, there have been few studies looking into this research topic in the HCI field. This paper presents a *Quaternary-Gaussian* model to quantitatively measure the endpoint uncertainty in crossing-based moving target selection. To validate this model, we conducted an experiment with discrete crossing tasks on five factors, i.e., initial distance, size, speed, orientation, and moving direction. Results showed that our model fit the data of μ and σ accurately with adjusted R^2 of 0.883 and 0.920. We also demonstrated the validity of our model in predicting error rates in crossing-based moving target selection. We concluded with a set of implications for future designs.

CSS Concepts
• Human-centered computing → Human computer interaction (HCI) → HCI theory, concepts and models

Author Keywords
Crossing-based Selection; Moving Target Selection; Endpoint Distribution; Error Rate

INTRODUCTION
Crossing-based selection [1, 4], by its meaning, refers to the way of selecting a target by crossing its boundary instead of pointing inside its perimeter. With the increasing popularity of novel input modalities such as pen [5], finger [21, 35] or in-air gesture [29], this crossing paradigm has gained increasing attention as it can adapt to these input modalities more naturally and can also improve user performance in particular scenarios.

CHI '20, April 25–30, 2020, Honolulu, HI, USA

ACM ISBN 978-1-4503-6708-0/20/04…$15.00
DOI: https://doi.org/10.1145/3313831.3376336

Interactive systems with dynamic contents, such as video games, augmented/virtual reality (AR/VR) systems and video surveillance applications are becoming ubiquitous nowadays. Moving target selection in these systems is a common yet challenging task, as pointing to a small and fast moving target would require high sensory-motor coordination of user [16, 17, 19]. Crossing paradigm may substitute or complement pointing as another fundamental interaction method in these systems as it selects the target with a dynamic gestures rather than clicks [2, 3]. Although moving target acquisition with crossing has already been adopted in many applications (e.g., the popular game *Fruit Ninja* [38], the well-known techniques CrossY [2] and AttachedShock [3]), there is still little understanding of human performance in crossing-based moving target acquisition in the HCI literature.

Modeling the uncertainty revealed by endpoint distribution of crossing-based moving target selection is essential to understand speed-accuracy trade-off and interaction efficiency in crossing-based user interfaces with dynamic contents. The endpoint in crossing-based selection is the location that the pointing device intersected with a target. With the advantage of such model, many unexplored questions can be solved, such as a) how likely are users to miss when they try to cross a target with a certain size and speed; b) how does the distribution of endpoints change with the size and speed of the target; c) is this change affected by the moving direction and the orientation of the target, and so on. This study aims to address such theoretical gap and comprehensively interpret the selection endpoints in HCI community.

There are three major challenges that we need to address for modeling the task. First, as the target is dynamic rather than static, the target speed brings additional effects on the endpoint uncertainty [17], which increases the complexity of the problem space. Second, target orientation and moving direction are important factors affecting the uncertainty in crossing-based moving target selection [5, 9]. The combination of these attributes generates a large number of conditions that need to be considered, which further

increases the difficulty of modeling. Third, the form and the coefficients of the model should be able to explain the speed-accuracy trade-off of user behavior in the task of crossing-based moving target selection, otherwise the significance of the model would be reduced.

This paper contributes a descriptive model and a set of empirical evidences that provide fundamental understanding for tasks involving moving target selection with crossing. Inspired by previous models and psychological evidences of human pointing movements [4, 6, 12, 17], we derived a *Quaternary-Gaussian* model to interpret the endpoint distribution in such tasks. We then conducted an experiment with discrete crossing tasks having 288 conditions generated based on 5 task factors (i.e., 2 initial distances, 3 target lengths, 3 target speeds, 8 moving directions and 2 target orientations). Results showed that the model fitted the empirical data well with 0.883 and 0.920 adjusted R^2 values for μ and σ respectively. By extending the model into an *Error-Model*, we observed good performances in predicting the error rates in crossing-based moving target selection. Finally, we concluded with implications derived from the model and empirical evidences for future designs.

RELATED WORK

We summarize existing studies related to modeling endpoint distribution in crossing-based moving target selection into three categories: crossing-based selection, moving target selection and endpoint uncertainty in moving target selection.

Crossing-based Selection

The first crossing study was conducted by Accot and Zhai during the process of deriving the well-known Steering law [4]. They found that the time to cross the goal can be determined by the distance and width of that goal. In their follow-up crossing study [5], they systematically evaluated two target-pointing tasks and four goal-crossing tasks which differ by the direction of the movement variability constraint (collinear vs. orthogonal) and by the nature of the action (pointing vs. crossing, discrete vs. continuous). They found that continuous crossing with collinear constraint (*C/CC*) is the slowest, while pointing and continuous crossing with orthogonal constraint (*OP* and *C/OC*) are at least 10% faster than other tasks. Discrete orthogonal crossing (*D/OC*) has the lowest error rate, and all crossing tasks have error rates close to or lower than pointing tasks except the task of *C/CC*.

Based on Accot and Zhai's original studies of crossing-based selection, researchers empirically evaluated the crossing selection performances on different input modalities and applications. Forlines and Balakrishnan [13] used Accot and Zhai's six tasks to study direct and indirect stylus inputs with tactile feedback. Luo and Vogel [21] also used the same six tasks to study crossing performance with direct touch input. They found that the *D/OC* task cannot be modeled accurately with standard Fitts' law. Instead, the "FFitts" law, which used endpoint uncertainty of finger to adjust Fitts' law prediction, can serve as a more accurate model for the task. This work inspired us to take endpoint uncertainty into account when modeling crossing-based moving target selection. Using a mouse and trackball, Wobbrock and Gajos [34] compared pointing and crossing with able-bodied people and those with motor impairments. By conducting two continuous studies on crossing-based selection, Apitz and Guimbretiere found evidences that crossing outperformed pointing in speed, and demonstrated the expressiveness of the crossing paradigm by implementing CrossY [2, 3]. While these studies show potential benefits for applying crossing paradigm in a wide range of applications, none of them systematically modeled the human performance regarding endpoint uncertainty of such tasks.

Moving Target Selection

A considerable amount of studies has been conducted to model moving target selection for predicting user performance. The model proposed by Jagacinski et al. [18] for movement time (*MT*) prediction in moving target selection is one of the well-known studies in this aspect. In the study, they extended the rule of speed-accuracy tradeoff reflected by Fitts' law [12, 37] to moving target selection by adding the term of speed into the Fitts' model. This work indicated that the initial distance barely affected the *MT* in position control systems. This result was consistent with the studies on dynamic targets with changing size. McGuffin and Balakrishnan [22], and Zhai et al. [36] suggested that the performance of Fitts' law is dominated by the final size of target when clicked, instead of the initial one. Hoffmann [15] proposed an alternative solution for *MT* prediction in moving target selection, by introducing the steady-state position error. Although these models predicted time duration rather than endpoint distribution, their results implied that the difficulty in moving target selection could increase as the moving speed of the target increased.

Moving target selection has also attracted much attention in the field of psychology. Tresilian [27] summarized six different types of pointing movements (i.e., pursuit, head-on, receding, perpendicular, pursuit + perpendicular and head-on + perpendicular), and developed a preprogrammed strategy for predicting *MT*. According to this study, we covered all these types of movements to evaluate the robustness of our model. Existing studies also showed that subjects tend to move their hand more quickly towards fast targets than slow ones [6, 10]. Together with the observed positive correlation of endpoint error to the speed of hand [12, 37], we inferred that, the selection uncertainty might be proportional to the target speed. Other evidences suggested that there is a time delay in the human sensory-motor system when users perform reaching movements [8, 14, 20, 26]. In our study, such time delay may also cause the endpoint to shift in the opposite direction of the target motion.

Human motor control studies aimed to understand organizing principles and processes behind people's movement actions. These studies suggested that human motor system resolves a complex set of dynamic during the

movement, and yields numerous possible trajectories [24, 25, 28, 30]. These models provided quality simulations to different properties (e.g. trajectories, profiles of speed and acceleration) of the reaching movement. However, they often required complex setting on the model structures and arguments, such as setting the locations or expected timestamps of via-points [25], weights of factors in the optimal goal [28, 30]. It is not convenient to use these models directly in HCI designs, due to the difficulties in tuning the arguments for practical uses [17].

Endpoint Uncertainty in Moving Target Selection

In contrast to the extensive studies on modeling *MT* in moving target selection in the HCI literature, very few studies have been carried out on understanding the endpoint distribution of such tasks.

One work focusing on the usage of endpoint distribution is the Temporal Pointing the usage of endpoint distribution is the Temporal Pointing [20]. The study presented a model to predict error rates in temporal pointing tasks with a temporal distance from beginning and a limited time window for selection. By combining perception process of visual cue into the model, the performance for modeling visual moving targets had been improved [19]. Nevertheless, the temporal pointing model is limited in considering the timing of hitting an approaching target solely, and the motion uncertainty of moving the cursor to intercept the target was omitted. It is reasonable to conclude that the endpoint distribution cannot be completely explained due to the case when only human time estimation is considered.

Recently, Huang et al. proposed a *Ternary-Gaussian* model, combining the movement uncertainty caused by motion and size of the target, to interpret endpoint uncertainty in selecting 1D moving targets [17]. The model assumed the endpoint distribution was a Gaussian distribution consisted of three Gaussian distributions, generated from uncertainties of input device, target length and the target speed. However, this model interpreted pointing rather than crossing movement. Moreover, it did not incorporate the effects of target moving direction and orientation on the endpoints. As these factors could lead to different movement strategies and user performances in crossing selection [5, 9, 27], it is necessary to take these factors into account when proposing a model for predicting the endpoint uncertainty in crossing-based moving target selection.

PROBLEM FORMULATION

In the task of crossing-based static target selection formulated by Accot and Zhai [5], the user is supposed to control a pointing device such as a mouse or stylus to cross a static target to trigger an action associated with the target. The task of crossing-based moving target selection inherits the same target selection paradigm of the static one, while allowing the target to move with certain speed and direction on the screen.

According to the work from Accot and Zhai, target selection with crossing can be divided into four patterns, distinguished by the need to lift the input device between two targets (discrete vs. continuous) and the orientation of the target with respect to the main direction of travel (collinear vs. orthogonal). For the first study on crossing-based moving target selection, we chose to focus on the patterns of discrete crossing selection, since it is ordinary for moving target selection and is more suitable compared to continuous crossing [21]. The orientation of the target was considered in this study due to its potential impact on endpoints when interacting with moving direction of the target. More specifically, the task of crossing-based moving target selection is formulated as follows:

As shown in Figure 1, firstly, users point on a starting point to trigger the task. After the task is triggered, a 1D goal (a bar) with a certain length appears on the screen and begins to move along a direction at a fixed speed. Then, users control a pointing device (e.g., a stylus) to cross the moving target for selection. This crossing task is discrete since the pointing device touches the screen only when crossing the goal; in the rest of the time the pointing device is lifted from the tablet surface. The task has five factors that may affect the crossing-based endpoint distribution on the target:

- Initial distance (*A*): the initial distance between the starting point and the target.
- Target length (*W*): the length of the target.
- Target speed (*V*): the moving speed of the target.
- Moving direction (*D*): the moving direction of the target.
- Target orientation (*O*): the orientation of the target.

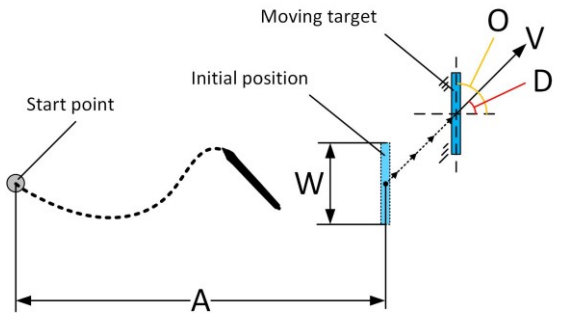

Figure 1. The task of crossing-based moving target selection

In the above task, an endpoint point is generated each time when the user attempts to cross the target. The endpoint is the location that the pointing device intersected with the target or the infinite line collinear with the target. By repeating the selection process, we can get a series of crossing endpoints, and then the problem that we try to solve in this study is formulated as finding a model to be descriptive of the distribution of these endpoints.

MODELING THE ENDPOINT DISTRIBUTION IN CROSSING-BASED MOVING TARGET SELECTION

To model the endpoint distribution in crossing-based moving target selection, we adopted the framework of the *Ternary-Gaussian* model [17] which has been demonstrated to accurately describe the endpoint distribution in pointing-based moving target selection.

Due to intrinsic differences between pointing and crossing interactions, we need to incorporate factors specifically related to the task of crossing-based moving target selection into our model. Apart from the nature of the movement and the form of the target included in the *Ternary-Gaussian* model, we also considered additional factors such as moving direction (D) and target orientation (O) that may significantly affect the endpoint distribution. We then defined a coordinate system to better characterize the endpoint locations in crossing-based moving target selection, and proposed a *Quaternary-Gaussian* model by decomposing a total motion component in the *Ternary-Gaussian* model into two independent components to suit the crossing movement.

Endpoint Coordinate System in Crossing-based Moving Target Selection

We used a local Cartesian coordinate system, with the origin fixed at the center of the target bar to describe the crossing endpoints in the task. The x-axis of the coordinate system was collinear with the bar, while the y-axis was perpendicular to one. To better describe the effects of target speed on the endpoints, the positive direction of the coordinate system is set to be always on the same side with the speed direction.

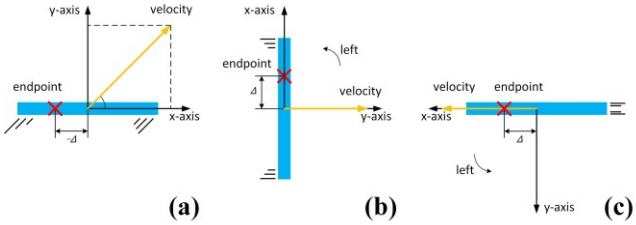

Figure 2. Examples for the coordinate system and associated endpoint values when the velocity is (a) inclined, (b) collinear and (c) perpendicular to the bar.

More specifically, the positive direction of each axis is determined by the direction of the velocity's projection on the axis. Figure 2 (a) shows an example that the velocity is inclined to the bar. Then the positive direction of x-axis follows the direction of the velocity's projection on it, which is the same for y-axis. When the velocity is perpendicular to an axis, the projection of it on this axis turns to be zero, without loss of generality, direction that rotates 90 degrees counterclockwise from the velocity is set as the positive direction of this axis. Figure 2 (b) and (c) reflects examples that the velocity is perpendicular x-axis and y-axis respectively.

According to this coordinate system, the crossing endpoints could only fall on x-axis, while the target velocity could have components on both x- and y- axis. The value of endpoint was a signed distance between the location of the endpoint and the center of the target at the time it was cross. There are three examples in the Figure 2, where endpoints are displayed, with the same distance from the target center and their corresponding values.

The Quaternary-Gaussian model

In the *Ternary-Gaussian* model [17], the endpoint distribution is described as a Gaussian distribution with three independent components, $X_a \sim N(\mu_a, \sigma_a^2)$, $X_s \sim N(\mu_s, \sigma_s^2)$ and $X_m \sim N(\mu_m, \sigma_m^2)$, corresponding to the **a**bsolute precision of the pointing device, the **s**ize of the target and the **m**otion of the target, respectively. Specifically, the location of the endpoints is a random variable X following a Gaussian distribution:

$$X \sim N(\mu, \sigma^2), \quad (1)$$

The endpoints X can be viewed as the sum of the three normally distributed components:

$$X = X_a + X_s + X_m \sim N(\mu, \sigma^2), \quad (2)$$

In order to adapt the *Ternary-Gaussian* model to describe the endpoint distribution in crossing-based selection, we adopted the definitions of absolute component and size component in the original model, and further decomposed the motion component according to the characteristics of crossing selection, obtaining two new components, collinear motion component and perpendicular motion component. By replacing the two components in Equation 2, we have the component expression of the *Quaternary-Gaussian* model:

$$X = X_a + X_s + X_{cm} + X_{pm} \sim N(\mu, \sigma^2), \quad (3)$$

We explain the four components as follows.

X_a is the absolute component, which is independent of users' intention to follow the specified task precision and cannot be controlled by a speed-accuracy tradeoff, hence the distribution parameters μ_a and σ_a are two constants.

X_s is the size component, which depends on the precision tolerance of the target. The precision requirement of selecting from users decreases due to the increase of the target size, thus the distribution parameters μ_s and σ_s of this component are proportional to the target size (W).

X_{cm} is the collinear motion component, which depends on the uncertainty caused by the collinear component of the target motion (i.e., velocity component in x-axis). There is a time delay in the human sensory-motor system when users try to reach targets. Such delay can vary among individuals and trials [8, 14, 20, 26]. This time delay affect the endpoint location through multiplying moving speed of the target. Therefore, the distribution parameters μ_{cm} and σ_{cm} of this component are proportional to the velocity component of the target in x-axis (V_x).

X_{pm} is the perpendicular motion component, which relies on the uncertainty caused by the perpendicular component of the target motion (i.e., velocity component in y-axis). The velocity component in y-axis cannot shift the endpoint

location directly, like the one in x-axis does. However, it affects the endpoint distribution through the accuracy loss of human hand in fast motion [6, 10], yielding a larger deviation and uncertain mean shift of endpoint distribution. Therefore, the distribution parameters μ_{pm} and σ_{pm} of this component are proportional to the velocity component of the target in y-axis (V_y).

Similar with *Ternary-Gaussian* model [17], when users try to select a target, they tend to use precision tolerance of the target (W) corresponding to the size component X_s, to compensate the sensory-motor delay corresponding to the collinear motion component X_{cm}. Therefore, the components of X_{cm} and X_s should had an interaction effect. We model this interaction effect of these two components by setting their covariance to a term V_x/W.

Afterwards, with the sum of the four Gaussian distributions, we have a total Gaussian distribution with parameter μ:

$$\begin{aligned}\mu &= \mu_a + \mu_s + \mu_{cm} + \mu_{pm}, \\ &= a + bW + cV_x + dV_y\end{aligned} \tag{4}$$

and parameter σ:

$$\begin{aligned}\sigma &= \sqrt{\sigma_a^2 + \sigma_s^2 + \sigma_{cm}^2 + \sigma_{pm}^2 + \mathrm{cov}(X_{cm}, X_s)} \\ &= \sqrt{e + fW^2 + gV_x^2 + hV_y^2 + i\frac{V_x}{W}}\end{aligned}. \tag{5}$$

Let θ represent the included angle between the velocity vector and the x-axis, we have $V_x = V\cos(\theta)$ and $V_y = V\sin(\theta)$. Then we have the final form of the *Quaternary-Gaussian* model is constructed:

$$\mu = a + bW + cV\cos(\theta) + dV\sin(\theta), \tag{6}$$

and,

$$\sigma = \sqrt{e + fW^2 + gV^2\cos^2(\theta) + hV^2\sin^2(\theta) + i\frac{V\cos(\theta)}{W}}. \tag{7}$$

Where, a, b, c, d, e, f, g, h and i are constants coefficients which can be measured via experiments. When $\theta = 0$, that is, the velocity vector is collinear to the bar, and no perpendicular velocity component, the *Quaternary-Gaussian* model reduces to the *Ternary-Gaussian* model.

The *Ternary-Gaussian* model was proposed based on three hypotheses, which were naturally adopted in the proposed *Quaternary-Gaussian* model. The three hypotheses are: **H1**: the endpoint distribution is Gaussian; **H2**: the initial distance (A) does not affect the endpoint distribution; **H3**: the target size (W) and the moving speed (V) affect the endpoint distribution. Although they have been validated in pointing-based moving target selection, it cannot be guaranteed that they are also valid in crossing-based selection. Therefore, in the next section, we empirically validate the above hypotheses and evaluate the *Quaternary-Gaussian* model.

STUDY 1: MODEL EVALUATION

In this section, we conducted a within-subject study to validate the model hypotheses and evaluate the proposed *Quaternary-Gaussian* model.

Participants and Apparatus

We recruited 15 subjects (9 females, with an average age of 23.4) in this study. All of them were right-handed and were familiar with the computer and stylus

The experiment was conducted on a Lenovo ThinkPad X1 laptop computer, with an Intel Core i7 8550 CPU at 1.8 GHz. A Wacom pen display and a stylus were used as input devices. The pen display was a direct interactive screen that can only be operated by stylus with 29.4 × 16.5 cm in size at 1920 × 1080 pixels resolution. Each pixel on the screen was 0.153 mm wide. The stylus was 15.4cm in length, 9mm in diameter at the barrel, and 10g in weight. The system ran with a sampling frequency of 100 Hz. The experiment programs were developed using Unity3D with C# code.

Design and Procedure

The experiment contained 288 conditions with four fully crossed factors including A, W, V, D and O as follow:

- Initial distance (A): 768 pixels and 1152 pixels
- Target length (W): 24 pixels, 48 pixels and 96 pixels
- Target speed (V): 96 pixels/sec, 192 pixels/sec and 384 pixels/sec
- Moving direction (D): 0°, 45°, 90°, 135°, 180°, 225°, 270° and 315°
- Target orientation (O): 0° and 90°

The above setting implicitly generated 3 levels (0°, 45° and 90°) of included angle (θ).

The settings of initial distance A, target length W and target speed V were referenced and selected from the settings of *Ternary-Gaussian* model [17]. The two relatively large distances were used to ensure that the moving target does not reach the user's cursor too quickly when moving toward the user (D = 180°). The target orientation of 0° and 90° corresponded to the collinear and orthogonal situations in Accot and Zhai's work [5]. The most representative eight moving directions in the four quadrants of Euclidean space were considered. The experiment had 2 blocks with 4 trials in each condition, resulting a total of 15 participants × 288 conditions × 4 trials × 2 blocks = 34,560 endpoints. The orders of all conditions in one block were randomized.

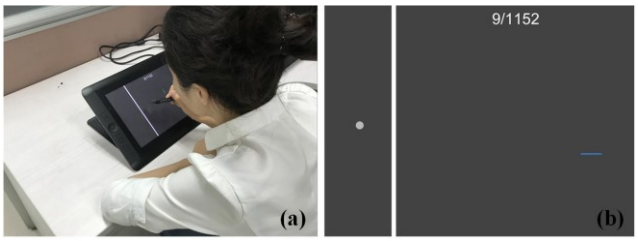

Figure 3. Experimental setting of this study.

In the experiment, participants seated in front of a table with their comfortable postures. The display was placed on center of the table with 30° inclination angle towards the participants, as shown in Figure 3 (a). Firstly, participants were informed about the purpose of the experiment, and were

allowed to perform practice trials until each participant explicitly expressed that s/he was ready to start. Each participant took about 100 minutes to finish the two blocks of the test. Rest were allowed between trials and blocks. Each participant was paid $30 for their time.

In each trial, a starting point (a small gray circle) first appeared near the left edge of the screen. The participant pointed on the starting point with the stylus to start. After a short delay (i.e., randomized from 200 - 600ms), a target appeared on the right side of the screen and began to move. The target was a blue bar with a certain length, which initially located on the same horizontal line as the starting point with a certain distance from it. The target moved as it appeared with a fixed speed. The participant was asked to cross the target as quickly and accurately as s/he could. An obstacle line was drawn between the starting point and the goal to remind the participants to use discrete strokes for crossing the target, as shown in Figure 3 (b). If the stroke of the participant did not intersect the target or the extension line at both ends of the target until the pen was lifted, the participant was asked to repeat the trial. Otherwise, no matter whether the participant hit the target, the coordinates of endpoint were recorded. If the pen tip missed the target, the endpoint was regarded as the point that the pen tip intersected with the infinite line collinear with the target.

Statistical Analysis

Normality Test

For the total 288 sets of endpoints, we removed the outliers (0.08% of the data) which the selection endpoint was more than twice the target length from the target center, followed similar approaches adopted by prior work. The majority of them (283 sets) passed the Kolmogorov-Smirnov test (*alpha*=.05) for normality of the distribution, which supported **H1**.

Effects of A, W, V, D, O and θ

To test the effects of task factors on endpoint distribution, we binned the endpoint data of *each* participant in each condition, yielding 4,320 sets of endpoint. By using maximum likelihood estimation (MLE) to get the actual distribution parameter (i.e., μ and σ) of these sets of endpoint, we got 4,320 pairs of μ and σ. Nonparametric Wilcoxon rank-sum test [31] is used for statistical tests as our μ and σ data were not normally distributed.

Results showed main effects of V ($\chi^2_{(2,N=4320)}$=1105.981, p<.001), D ($\chi^2_{(7,N=4320)}$=26.311, p<.001), O ($\chi^2_{(1,N=4320)}$=108.386, p<.001) and θ ($\chi^2_{(1,N=4320)}$=704.359, p<.001) on μ. The effect of W ($\chi^2_{(2,N=4320)}$=2.707, p=.067) was marginally significant. No significant main effect of A ($\chi^2_{(1,N=4320)}$=0.006, p=.941) was found.

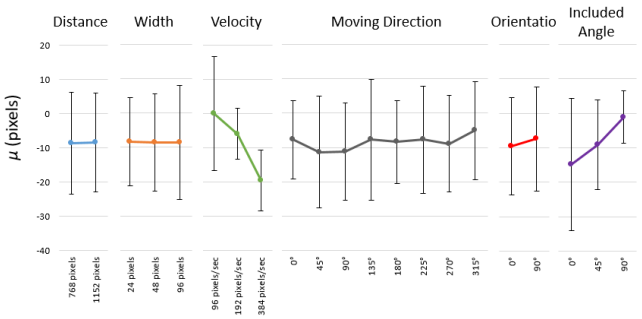

Figure 4. Average μ in each level of the task factors. Error bars represent the standard deviations.

The average μ in each level of the factors are shown in Figure 4. For speed (V), the average μ at condition of V=96 pixels/sec was almost zero (0.043 pixels), followed by larger negative value at condition of V=192 pixels/sec (-5.969 pixels), and at condition of V=384 pixels/sec (-19.634 pixels). The target motion is shifting the mean of endpoint in contrast to the moving direction, and higher speed results in larger shift. For moving direction (D), under the conditions of D=270° and D=315°, the average μ had the highest negative values of -11.331 and -11.295 pixels. In other cases, this value ranged from -8.889 to -5.049 pixels, with the lowest value at D=180°. For target orientation (O), we observed a larger average negative μ at the condition of O=0° (-9.585 pixels) then O=90° (-7.455 pixels). For included angle (θ), the average μ had the highest negative value at condition of θ=0° (-14.857 pixels), followed by condition of θ=45° (-9.076 pixels) and it turned down to almost zero at condition of θ=90° (-1.069 pixels).

Main effects of W ($\chi^2_{(2,N=4320)}$=227.156, p<.001), V ($\chi^2_{(2,N=4320)}$=293.903, p<.001), D ($\chi^2_{(7,N=4320)}$=13.223, p<.001), and O ($\chi^2_{(1,N=4320)}$=120.020, p<.001) were found on σ. No significant main effect of A ($\chi^2_{(1,N=4320)}$=1.877, p=.171) was observed.

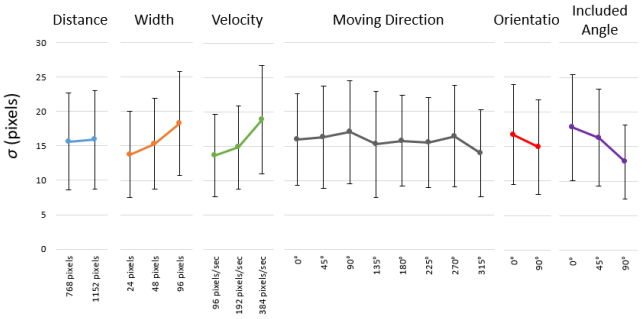

Figure 5. Average σ in each level of the task factors. Error bars represent the standard deviations.

The average σ in each level of the factors were shown in Figure 5. For width (W), the average σ at condition of W=96 pixels was the largest (18.299 pixels), followed by condition of W=48 pixels (15.299 pixels), and condition of W=24 pixels (13.757 pixels). For speed (V), the average σ at condition of V=384 pixels/sec was the largest (18.874 pixels), followed by condition of V=192 pixels/sec (14.837 pixels), and

condition of V=96 pixels/sec (13.639 pixels). For moving direction (D), the conditions of D=90° and D=270° had the first and second largest average σ of 17.011 pixels and 16.435 pixels, while the lowest was the condition of D=315° with 13.968 pixels. In other cases, the values ranged from 15.267 pixels to 16.321 pixels. It seemed that the standard deviation of endpoint distribution in the two vertical directions is larger. For target orientation (O), a larger average σ at the condition of O=0° (16.704 pixels) then O=90° (14.862 pixels) was observed. For included angle (θ), the condition of θ=0° had the highest average σ (17.763 pixels), followed by condition of θ=45° (16.297 pixels) and condition of θ=90° (12.776 pixels).

According to the results, the initial distance A did not have a significant effect on endpoint distribution, which supported **H2**. Both of the target length W and the moving speed V significantly affected the endpoint distribution, which supported **H3**. The endpoint uncertainty was increased (i.e., higher offsets or variations of endpoints) as W and V increased in crossing-based moving target selection, which was consistent with prior *Ternary-Gaussian* model in pointing moving targets [17]. The target orientation also exhibited significant effects on endpoint uncertainty, where, the endpoint offset and variations were larger in the condition of O=0°. There was no clear trend of the influence of moving direction on the endpoint uncertainty was found. Comparatively, the factor θ derived from O and D had a clear trend affecting the endpoint uncertainty. This result indicated θ a more sensitive factor, which was adopted in the model.

Correlation Analysis

To further investigate the relationships between task factors and the endpoint distribution, we binned endpoint data of *all* participants in each condition, yielding 288 sets of endpoint, and then Pearson correlations were calculated between the μ and σ (N=288) and each of the 6 task factors as showed in Table 1.

Factors	μ	σ
A	.009	.030
W	-.007	.410**
V	-.711**	.580**
D	.097	-.106
O	.091	-.193**
θ	-.422**	-.454**

Table 1. Correlations between task factors and μ and σ of the endpoint distributions. "" indicates correlations with significance levels above 99%.**

Results showed that V and θ were significant correlations to μ, and the correlation coefficients between the two pairs were negative. The correlations between pairs of A and μ, W and μ, D and μ, O and μ did not achieved significant levels as we expected. We found more task factors were significantly correlated to the standard deviation of endpoints, where W and V were positive correlated to σ and, O and θ were negative correlated. The correlation coefficient between O and σ was relative small (<0.3). A and D were not significant correlated to σ.

The results of correlation analysis were highly consistent with the Wilcoxon rank-sum test on our data. Changing the initial distance did not lead to a significant change of the endpoint distribution, while the target length and moving speed did. **H2** and **H3** were further validated. The influence of moving direction on endpoint distribution did not achieve significant level, and target orientation only showed a relatively weak influence on the distribution range. On the contrast, a strong correlation was found between θ and the endpoint distribution, which further demonstrated that the factor θ strong indicator for endpoint distribution.

Model Evaluation

In this section, we tested the fitting precision of the proposed *Quaternary-Gaussian* model within two data binning conditions including $W \times V \times \theta$ condition (N=27) and $A \times W \times V \times D \times O$ condition (N=288).

Measures

Three measurements were used to evaluate our model, including adjusted R^2, mean absolute error (MAE), and mean Wasserstein distance (MWD). Wasserstein distance [4] is a statistical distance defined between two probability distributions. Intuitively, the metric is the minimum "cost" of turning one pile (distribution) into the other. The mean of Wasserstein distance (i.e., MWD) is the average Wasserstein distance from actual distributions to the predicted distributions across all conditions, it ranged from 0 to positive infinity, and a smaller MWD indicates a higher fitting score. MWD provide one overall fitting score for a Gaussian distribution rather than measure μ and σ separately with adjusted R^2 and MAE.

We used the `nlinfit` function provided in `MATLAB` to estimate each coefficient of the *Quaternary-Gaussian* model, and computed the measurements of adjusted R^2, MAE and MWD for the two data binning conditions. Performances of the prior *Ternary-Gaussian* model [17] on our data set were provided as a baseline.

$W \times V \times \theta$ Condition

In the $W \times V \times \theta$ condition, similar with other Fitts' law studies [4, 5, 12], we binned the endpoint data with the explicit factors W, V and θ in the model. There were 27 $W \times V \times \theta$ combinations, thus we got 27 pairs of μ and σ to for model fitting.

Model	Para.	Adj. R^2	MAE	MWD
Ternary-Gaussian	μ	0.381	5.429	71.486
	σ	0.474	2.231	
Quaternary-Gaussian	μ	0.883	3.112	13.480
	σ	0.920	0.924	

Table 2. The fitting performances of the *Ternary-Gaussian* and our models in the $W \times V \times \theta$ condition (N=27).

As shown Table 2, our model fitted the empirical data well with 0.883 and 0.920 adjusted R^2 for μ and σ respectively, which were much higher than those of the *Ternary-Gaussian* model (0.381 and 0.474). The MAEs of our model for μ and σ were 3.112 pixels and 0.924 pixels respectively, which were only about half of those in the *Ternary-Gaussian* model. Is meaned that the average error between the predicted and actual mean of endpoints was about 3 pixels, and it was less than 1 pixel for the standard deviation of endpoints. MWDs of the two models reflected similar results. The 13.480 MWD of our model indicated a very small distance between the predicted and actual endpoint distribution on average.

In Figure 6, all predicted (dash line) and actual (colored solid line) endpoint distributions in the 27 conditions were plotted and mapped on associated targets. The targets were plotted with the positive direction of x-axis up-forwarded. For each row in Figure 6, the vertical axis was the axis of endpoint and the horizontal axis was a categorical axis mapped with three V conditions ascendingly. The three θ conditions were marked by different colors. A straight line was drawn on the center of endpoint distributions to mark the μ values of them. Obviously, all the predicted endpoint distributions were vary closed to the actual data.

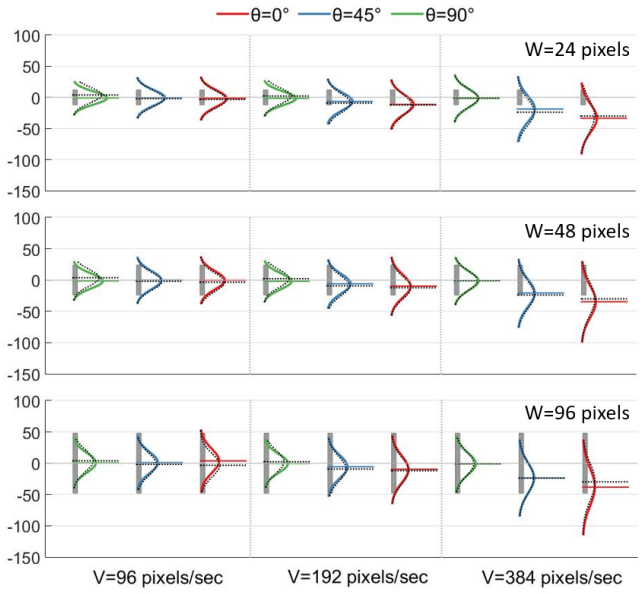

Figure 6. The estimated (dash line) and actual (colored solid line) endpoint distributions mapped on the targets.

A × W × V × D × O Condition

In the second condition, we binned the endpoint data with the original factors A, W, V, D and O, yielding 288 $A \times W \times V \times D \times O$ combinations and 288 pairs of μ and σ accordingly.

As illustrated in Table 3, in the $A \times W \times V \times D \times O$ condition, the adjusted R^2 for μ and σ were 0.816 and 0.747, and the MAEs for μ and σ were 3.92 pixels and 1.974 pixels respectively, resulting a MWD score of 24.477. Again, our model outperformed the *Ternary-Gaussian* model in the three measurements. Although the performances of our model were reduced, considering the larger number of data point (N=288 vs. N=27), these results were still acceptable. Comparing with the $W \times V \times \theta$ condition, the main gaps came from the lower fitting for σ. Such results indicated that although the factor θ had captured most of the effects of A, D and O on the mean of endpoints, it did not completely cover their effects on the distribution range of endpoints. Together with the results of our statistical analysis, we could infer that the orientation of the target had a significant effect on standard deviation of endpoints that worked independently from θ. This phenomenon was consistent with Accot and Zhai's study in acquiring static targets with crossing [5], where higher uncertainty of endpoints was observed when participants tried to acquire targets collinear (i.e., O=0°) to the reaching movements.

Model	Para.	Adj. R^2	MAE	MWD
Ternary-Gaussian	μ	0.498	5.502	66.998
	σ	0.479	2.717	
Quaternary-Gaussian	μ	0.816	3.926	24.477
	σ	0.747	1.974	

Table 3. The fitting performances of the *Ternary-Gaussian* and our models in the $A \times W \times V \times D \times O$ condition (N=288).

Model Coefficients

The coefficients of the model fitted by the data in $W \times V \times \theta$ condition were showed in Table 4. These coefficients reflect the relationship of each term of the model (i.e., W, V_x, V_y and V_x/W) on endpoints distribution.

Para.	Coeff.	Term	Estimated
μ	a	-	5.2710
	b	W	0.0018
	c	V_x	-0.0917
	d	V_y	-0.0160
σ	e	-	141.6022
	f	W	0.0194
	g	V_x	0.0037
	h	V_y	0.0004
	i	V_x/W	0.0003

Table 4. The coefficients of our model fitted by the data in the $W \times V \times \theta$ condition.

From coefficients of μ, we learned that the values of c and d were negative, indicated that both V_x and V_y made the mean of endpoints shift in the opposite direction to the moving direction. The absolute value of c were larger than d indicated that V_x contributed more on shifting the endpoints than V_y. The positive b values were consistent with our assumption that user tend to used W to compensate the shift of μ. From coefficients of σ, we learned that the distribution range of endpoints increased as W, V_x and V_y increased. We found

larger value of g than h, indicating that V_x contributed more on increasing σ than V_y did. The term V_x/W also contributed to increased σ, however, as the value of i is relative small, the contribution of this term on σ was almost negligible.

STUDY 2: PREDICTING USER PERFORMANCE WITH THE MODEL

Error rate is one of the most important factors of user performance in HCI [17, 19, 33]. It would be helpful for crossing-based interface design if we know the likelihood of missing a target when they try to cross it with a certain size and speed. With the *Quaternary-Gaussian* model, we can estimate the error rate via cumulative distribution function (CDF) for crossing-based moving target selection. The CDF of the Gaussian distribution specified by μ and σ is:

$$P(x) = \frac{1}{\sigma\sqrt{2\pi}} \int_{-\infty}^{x} \exp\left(-\frac{(x-\mu)^2}{2\sigma^2}\right) \quad (8)$$

The following equation shows the probability that X falls into the range of $(-\infty, x)$:

$$P(x) = \frac{1}{2}\left[1 + erf\left(\frac{x-\mu}{\sigma\sqrt{2}}\right)\right] \quad (9)$$

where erf(x) is the error function encountered in integrating the normal distribution. The error rate is the probability that X falls out of the range (x_0, x_1), where x_0 and x_1 represent the boundaries of the target:

$$\begin{aligned} ER(\mu,\sigma) &= 1 - [P(x_1) - P(x_0)] \\ &= 1 - \frac{1}{2}\left[erf\left(\frac{x_1-\mu}{\sigma\sqrt{2}}\right) - erf\left(\frac{x_0-\mu}{\sigma\sqrt{2}}\right)\right] \end{aligned} \quad (10)$$

where μ and σ are defined by our model. We denote Equation (10) as the *Error-Model* founded on the *Quaternary-Gaussian* model. We then used the data in previous section to evaluate the goodness of fit and the generalizability of the *Error-Model*.

The *Error-Model* fitted the data of error rate well with 0.964 adjusted R^2 and MAE 3.2%. A repeated three-fold cross-validation was conducted to test the generalizability of the *Error-Model*. The model coefficients were obtained over the data of 10 randomly chosen subjects and tested on the rest 5. Over 100 iterations, we obtain an average MAE of 5.7% (SD=1.2), indicating the model can safely be generalized between similar populations.

We plotted the estimated and actual error rates for all 27 conditions in Figure 7. We could infer from the figure that the error rates increased when the speed (V) increased, and when the size (W) and the include angle (θ) decreased. Apparently, increasing target speed and decreasing include angle increased the offset and variation of endpoints, thus increasing the selection error rate. However, increasing target size also increased the variation of endpoints but it decreased the error rate instead. This is because, on the one hand, increasing the target size increased the range for successful selection, which was revealed in Equation 10; on the other hand, larger target size compensated the effect of target speed on endpoint uncertainty, as it had been showed in Equation 7.

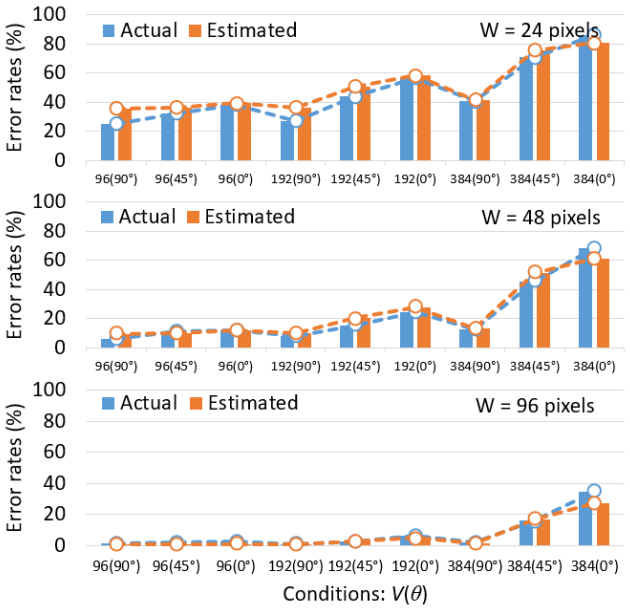

Figure 7. The estimated and actual error rates in all the 27 conditions.

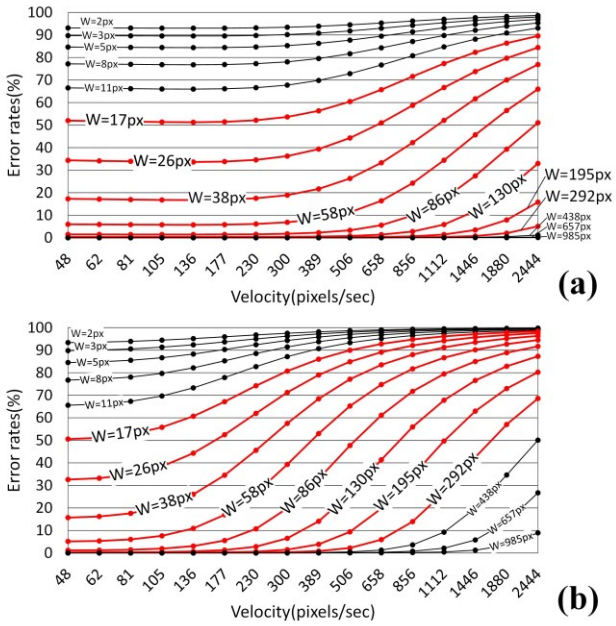

Figure 8. Error rate spectrums in the conditions of a) $\theta = 90°$ and b) $\theta = 0°$.

The model predicts errors as a function of how difficult the selection task is. The difficulty of the task would increase if the target moves faster or the size of it is smaller. By changing V and W in a wider range of values, we can get an "error rate spectrum" reflecting effects of V and W on the error rates of crossing selection. We selected a V in the range of 48 to 2444 pixels/sec (7.34 to 373.92 mm/sec), and a W in the range of 0 to 985 pixels (0 to 150.70 mm) to illustrate the spectrum (Figure 8). Referencing experimental settings in previous works [7, 21, 37], curves of the most studied target

sizes ranged from 17 to 195 pixels (2.6 to 29.83 mm) were marked red to better presents the spectrum.

Consistent with prior observations, the spectrum shows that error rate increases as target size decreases, and as target speed increases. It can also be seen from the spectrum that error rates in the condition of $\theta = 0°$ increase faster than that in the condition of $\theta = 90°$. In addition, targets with a size smaller than 17 pixels (2.60 mm) always have 50% or higher error rates. For $\theta = 90°$ condition, the error rate is dominated by target size when target speed is lower than 177 pixels/sec (27.08 mm/sec), and this threshold goes down to 48 pixels/sec (7.34 mm/sec) in $\theta = 0°$ condition. We also found that, for $\theta = 90°$ condition, when the target size is larger than 292 pixels (44.67 mm), users rarely miss the target (error rate < 10%), and this threshold goes up to 985 pixels 150.70 mm in $\theta = 0°$ condition. In both conditions of $\theta = 90°$ and $\theta = 0°$, the targets with size range from 26 to 195 pixels (3.97 to 29.83 mm) show rich variety across all commonly used conditions.

DESIGN IMPLICATIONS AND TAKEAWAYS

Based on the empirical evidences in this study, we summarized following implications and takeaways that could be helpful for creating user interfaces involve dynamic crossing targets:

1) Initial distance does not affect significantly to endpoint uncertainty. Therefore, in most cases, when considering increasing selection accuracy, designers should not worry about the distance of the target, but try to increase the target size and slow down the target speed.

2) Included angle of velocity and the target play an important role affecting the endpoint uncertainty in crossing-based moving selection. In a particular situation, crossing-based moving targets with a velocity collinear to the targets have a higher selection difficulty than the ones with a velocity perpendicular to them. Thus, keeping the velocity perpendicular or approximately perpendicular to the target is a good choice for including the selection accuracy for designers.

3) When users attempt to acquire targets that are collinear with the reaching movement, the selection difficulty is higher than that when the target is perpendicular to the reaching movement. Thus, when it's impossible to change the direction of target velocity to make it perpendicular to the target as suggested in (2), changing the orientation of the target to make it perpendicular to the users' reaching movement is also worth considering.

4) Given the error rate spectrum, in the condition that the target velocity is perpendicular to the target, the error rate is dominated by only the target size (i.e., can be treated as static target) when the speed is lower than 27.08 mm/sec, and this threshold goes down to 7.34 mm/sec in the condition that target velocity is collinear to it. Accordingly, in any case, adding a moving speed of less than 7.34 mm/sec to an selectable target will not have a significant impact on its selection difficulty.

5) The error rate spectrum also indicated that, in the condition that the target velocity is perpendicular to the target, when the target size is larger than 44.67 mm, users rarely miss the target, and this threshold goes up to 150.70 mm in the condition that target velocity is collinear to it. Therefore, when a target is larger than 150.70 mm, adding any moving speed in a reasonable range (i.e., lower than 373.92 mm/sec) will not have a significant impact on its selection difficulty.

6) Given the reasonable range of velocity (i.e., lower than 373.92 mm/sec). The selection difficulty of targets with sizes ranging from 3.97 mm to 29.83 mm highly depended on target velocity. For example, the error rates of targets with size of 3.97 mm varied from nearly 35% to 100%, but the ones with size of 2.60 mm could not be lower than 50%. This suggest we can choose this size range for certain tasks that requires the dynamic adaptation of difficulty levels, such as controlling the level of challenge in games with crossing selection as the main interaction paradigm.

CONCLUSION

In this paper, a model that can precisely describe the distribution of the endpoints in crossing-based moving target selection is presented. An experiment was carried out to validate the model. Results showed that this model fits the empirical data well and showed robustness across conditions. The form and coefficients of the model reveals the regularities of the crossing movement in dynamic targets. When using our model to estimate error rates, we observed high fitting results and generalizability. Finally, we summarized a set of implications for future design based on the empirical data from this study.

This paper did not consider the type of continuous crossing-based selection. The consecutive movement in continuous crossing selection task may introduce higher uncertainty to the endpoint distribution. If this assumption is true, it is very interesting to find out the underlaying mechanism of this phenomenon. In addition, we observed a significant effect of target's orientation on endpoint distribution, which seems to be independent of W, V and θ. In-depth and systematic research on the effects of target orientation on endpoint distribution is needed. In the future, we are interested in extending our research in other user interfaces such as touch screen and eye tracking. We are also interested in exploring how our model can help improve interface design in real-world applications such as VR applications and games.

ACKNOWLEDGMENTS

This work was supported by the National Key R&D Program of China (Grant No. 2016YFB1001405), the National Natural Science Foundation of China (Grant No. 61802379, 61602236), and Youth Innovation Promotion Association CAS.

REFERENCES

[1] Johnny Accot. 2001. *Les Tâches Trajectorielles en Interaction Homme-Machine—Cas des tâches de navigation.* Ph.D Dissertation. Université de Toulouse 1.

[2] Georg Apitz and François Guimbretière. 2004. CrossY: a crossing-based drawing application. In *Proceedings of the 17th annual ACM symposium on User interface software and technology* (UIST '04), 3-12. http://dx.doi.org/10.1145/1029632.1029635

[3] Georg Apitz, François Guimbretière, and Shumin Zhai. (2008). Foundations for designing and evaluating user interfaces based on the crossing paradigm. *ACM Transactions on Computer-Human Interaction*, 17, 2 (May 2008), 42. https://doi.org/10.1145/1746259.1746263

[4] Johnny Accot and Shumin Zhai. 1997. Beyond Fitts' law: models for trajectory-based HCI tasks. In *Proceedings of the SIGCHI Conference on Human Factors in Computing Systems* (CHI'97). 295–302. http://dx.doi.org/10.1145/1120212.1120376

[5] Johnny Accot and Shumin Zhai. 2002. More than dotting the i's ---foundations for crossing-based interfaces. In *Proceedings of the SIGCHI Conference on Human Factors in Computing Systems* (CHI '02), 73–80. http://dx.doi.org/10.1145/503376.503390

[6] Phillip J. Bairstow. 1987. Analysis of hand movement to moving targets. *Human Movement Science*, 6, 3(1987), 205-231. http://dx.doi.org/10.1016/0167-9457(87)90013-3

[7] Xiaojun Bi, Yang Li and Shumin Zhai. 2013. FFitts law: modeling finger touch with fitts' law. In *Proceedings of the SIGCHI Conference on Human Factors in Computing Systems* (CHI '13), 1363-1372. http://dx.doi.org/10.1145/2470654.2466180

[8] Eli Brenner, Jeroen B. J. Smeets. 1996. Hitting moving targets: Co-operative control of 'when' and 'where'. *Human Movement Science*, 15, 1(1996), 39–53. http://dx.doi.org/ 10.1016/0167-9457(95)00036-4

[9] Eli Brenner, Jeroen B. J. Smeets. 2007. Flexibility in intercepting moving objects. *Journal of Vision*, 7, 5(2007), 1-17. http://dx.doi.org/10.1167/7.5.14

[10] Reinoud J. Bootsma and Piet C. W. van Wieringen. 1990. Timing an attacking forehand drive in table tennis. *Journal of experimental psychology: Human perception and performance*, 16, 1(1990), 21-29. http://dx.doi.org/10.1037//0096-1523.16.1.21

[11] Xiaojun Bi and Shumin Zhai. 2013. Bayesian touch: a statistical criterion of target selection with finger touch. In *Proceedings of the 26th annual ACM symposium on User interface software and technology* (UIST '13), 51-60. http://dx.doi.org/10.1145/2501988.2502058

[12] Paul M Fitts. 1954. The information capacity of the human motor system in controlling the amplitude of movement. *Journal of experimental psychology*, 47, 6 (Jun 1954), 381-391. http://dx.doi.org/10.1037/h0055392

[13] Clifton Forlines and Ravin Balakrishnan. 2008. Evaluating tactile feedback and direct vs. indirect stylus input in pointing and crossing selection tasks. In *Proceedings of the SIGCHI Conference on Human Factors in Computing Systems* (CHI '08), 1563–1572. http://dx.doi.org/10.1145/1357054.1357299

[14] David W. Franklin and Daniel M. Wolpert. 2011. Computational Mechanisms of Sensorimotor Control. *Neuron*, 72, 3 (2011), 425-442. http://dx.doi.org/10.1016/j.neuron.2011.10.006

[15] Errol R. Hoffmann. 1991. Capture of moving targets: a modification of Fitts' Law. *Ergonomics*, 34, 2(1991), 211-220. http://dx.doi.org/10.1080/00140139108967307

[16] Khalad Hasan, Tovi Grossman, and Pourang Irani. 2011 Comet and target ghost: techniques for selecting moving targets. In *Proceedings of the SIGCHI Conference on Human Factors in Computing Systems* (CHI '11), 839-848. http://dx.doi.org/10.1145/1978942.1979065

[17] Jin Huang, Feng Tian, Xiangmin Fan, Xiaolong (Luke) Zhang, and Shumin Zhai. 2018. Understanding the Uncertainty in 1D Unidirectional Moving Target Selection. In *Proceedings of the 2018 CHI Conference on Human Factors in Computing Systems* (CHI '18), Paper 237, 1-12. https://doi.org/10.1145/3173574.3173811

[18] Richard J. Jagacinski, Daniel W. Repperger, Sharon L. Ward and Martin S. Moran. 1980. A test of Fitts' law with moving targets. *Human Factors: The Journal of the Human Factors and Ergonomics Society*, 22, 2 (April 1980), 225-233. http://dx.doi.org/10.1177/001872088002200211

[19] Byungjoo Lee, Sunjun Kim, Antti Oulasvirta, Jong-In Lee, and Eunji Park. 2018. Moving Target Selection: A Cue Integration Model. In *Proceedings of the 2018 CHI Conference on Human Factors in Computing Systems* (CHI '18), Paper 230, 1-12. http://dx.doi.org/10.1145/3173574.3173804

[20] Byungjoo Lee and Antti Oulasvirta. 2016. Modelling Error Rates in Temporal Pointing. In *Proceedings of the 2016 CHI Conference on Human Factors in Computing Systems* (CHI '16), 1857-1868. http://dx.doi.org/10.1145/2858036.2858143

[21] Yuexing Luo and Daniel Vogel. 2014. Crossing-based selection with direct touch input. In *Proceedings of the SIGCHI Conference on Human Factors in Computing Systems* (CHI '14), 2627-2636. http://dx.doi.org/10.1145/2556288.2557397

[22] Michael McGuffin and Ravin Balakrishnan. 2002. Acquisition of expanding targets. In *Proceedings of the SIGCHI Conference on Human Factors in Computing Systems* (CHI '02), 57-64. http://dx.doi.org/10.1145/503376.503388

[23] I. Scott MacKenzie, Abigail Sellen and William A. S. Buxton. 1991. A comparison of input devices in elemental pointing and dragging tasks. In *Proceedings of the SIGCHI Conference on Human Factors in Computing Systems* (CHI '91), 161-166. http://dx.doi.org/10.1145/108844.108868

[24] Ning Qian, Yu Jiang, Zhongping Jiang and Pietro Mazzoni. 2013. Movement duration, fitts's law, and an infinite-horizon optimal feedback control model for biological motor systems. *Neural Computation*. 25, 3 (March 2013), 697-724. http://dx.doi.org/10.1162/NECO_a_00410

[25] Philip Quinn and Shumin Zhai. 2018. Modeling Gesture-Typing Movements. *Human-Computer Interaction*, 33, 3(2018), 234-280. http://dx.doi.org/10.1080/07370024.2016.1215922

[26] Gabor Stepan. 2009. Delay effects in the human sensory system during balancing. *Philosophical transactions. Series A, Mathematical, physical, and engineering sciences*. 367 (2009). 1195-1212. https://doi.org/10.1098/rsta.2008.0278

[27] James R. Tresilian. 2005. Hitting a moving target: Perception and action in the timing of rapid interceptions. *Perception & Psychophysics*, 67, 1 (January 2005), 129-149. http://dx.doi.org/10.3758/BF03195017

[28] Emanuel Todorov. 2005. Stochastic optimal control and estimation methods adapted to the noise characteristics of the sensorimotor system. *Neural Computation.* 17, 5, (May 2005), 1084-1108. http://dx.doi.org/10.1162/0899766053491887

[29] Huawei Tu, Susu Huang, Jiabin Yuan, Xiangshi Ren, and Feng Tian. 2019. Crossing-Based Selection with Virtual Reality Head-Mounted Displays. In *Proceedings of the SIGCHI Conference on Human Factors in Computing Systems* (CHI '19), paper 618, 1-14. http://dx.doi.org/10.1145/3290605.3300848

[30] Emanuel Todorov and Michael I. Jordan. 2002. Optimal feedback control as a theory of motor coordination. *Nature Neuroscience*. 5, 11 (November 2002), 1226-1235. http://dx.doi.org/10.1038/nn963

[31] Frank Wilcoxon. 1945. Individual comparisons by ranking methods. *Biometrics Bulletin*, 1 (6), 80-83. http://dx.doi.org/10.1007/978-1-4612-4380-9_16

[32] L. N. Wasserstein. 1969. Markov Processes on Countable Space Product Describing Large Systems of Automata. *Problemy. Peredachi. Informatsii.* 5:3 (1969), 64-73. (in Russian)

[33] Jacob O. Wobbrock, Edward Cutrell, Susumu Harada, and I. Scott MacKenzie. 2008. An error model for pointing based on Fitts' law. In *Proceedings of the SIGCHI Conference on Human Factors in Computing Systems* (CHI '08), 1613-1622. http://dx.doi.org/10.1145/1357054.1357306

[34] Jacob O. Wobbrock and Krzysztof Z. Gajos. 2008. Goal Crossing with Mice and Trackballs for People with Motor Impairments: Performance, Submovements, and Design Directions. *ACM Transactions on Accessible Computing*, 1, 1 (2008), 4:1–4:37. http://dx.doi.org/10.1145/1361203.1361207

[35] Chuang-Wen You, Yung-Huan Hsieh, Wen-Huang Cheng and Yi-Hsuan Hsieh. 2014. AttachedShock: Design of a crossing-based target selection technique on augmented reality devices and its implications. *International Journal of Human-computer Studies*, 72, 7 (2014), 606-626. http://dx.doi.org/10.1016/j.ijhcs.2014.03.001

[36] Shumin Zhai, Stéphane Conversy, Michel Beaudouin-Lafon and Yves Guiard. 2003. Human on-line response to target expansion. In *Proceedings of the SIGCHI Conference on Human Factors in Computing Systems* (CHI '03), 177-184. http://dx.doi.org/10.1145/642611.642644

[37] Shumin Zhai, Jing Kong and Xiangshi Ren. 2004. Speed–accuracy tradeoff in Fitts' law tasks—on the equivalency of actual and nominal pointing precision. *International Journal of Human-Computer Studies*, 61, 6 (December 2004), 823-856. http://dx.doi.org/10.1016/j.ijhcs.2004.09.007

[38] Fruit Ninja. https://fruitninja.com/